Phase Separation Scenario for Manganese Oxides and Related Materials

Adriana Moreo, Seiji Yunoki, Elbio Dagotto

Recent computational studies of models for manganese oxides have revealed a rich phase diagram, which was not anticipated in early calculations in this context performed in the 1950s and 1960s. In particular, the transition between the antiferromagnetic insulator state of the hole-undoped limit and the ferromagnetic metal at finite hole density was found to occur through a mixed-phase process. When extended Coulomb interactions are included, a microscopically charged inhomogeneous state should be stabilized. These phase separation tendencies, also present at low electronic densities, influence the properties of the ferromagnetic region by increasing charge fluctuations. Experimental data reviewed here by applying several techniques for manganites and other materials are consistent with this scenario. Similarities with results previously discussed in the context of cuprates are clear from this analysis, although the phase segregation tendencies in manganites appear stronger.

Hole-doped manganese oxides with a perovskite structure have stimulated considerable scientific and technological interest because of their exotic electronic and magnetic properties (*1*). These manganites have chemical composition $R_{1-x}A_xMnO_3$, where R is a rare-earth ion and A is a divalent ion such as Ca, Sr, Ba, or Pb. They present an unusual magnetoresistance (MR) effect, whereby magnetic fields induce large changes in their resistivity, ρ, a property that may find applications in sensor technologies such as that utilized in magnetic storage devices. For example, in La-Ca-Mn-O thin films, the ratio $[\rho(0) - \rho(H)]/\rho(H)$, where $\rho(H)$ is the resistivity in magnetic field H, can be as large as 10^3 at 77 K ($H = 6$T). The term colossal MR (CMR) has been coined to describe this effect (*2*).

The unusual properties of manganese oxides challenge our current understanding of transition-metal oxides and define a basic research problem that involves an interplay between the charge, spin, phononic, and orbital degrees of freedom. Manganites have a rich phase diagram (*3*) that includes a well-known ferromagnetic (FM) phase that spans a robust range of electronic densities. The CMR effects have been observed particularly at small hole densities x but also at $x \sim 0.5$, which are the density limits of the FM phase. The strength of the MR effect increases as the electronic bandwidth is decreased through chemical substitution (*1*), which also reduces the Curie critical temperature T_C. At hole concentrations $x \sim 0.5$, an anti-FM (AF) charge-ordered (CO) insulating state, discussed by Goodenough (*4*), is involved in the CMR effect, which at these densities is extraordinarily large (*5*).

In the undoped limit, the Mn^{3+} ions have four electrons in the 3*d* shell, and they are surrounded by oxygens O^{2-}, forming an octahedron. This crystal environment breaks the full rotational invariance, causing the two e_g and three t_{2g} orbitals to split. The strong Hund coupling (J_H) in these systems favors the spin alignment of the four electrons in the active shell; on average three electrons populate the t_{2g} orbitals and one occupies the e_g states. The t_{2g} electrons are mainly localized, whereas the e_g electrons are mobile and use O *p* orbitals as a bridge between Mn ions. When the manganites are doped with holes through chemical substitution, Mn^{4+} ions with only three t_{2g} electrons are formed. In addition, in the undoped limit the e_g degeneracy is split due to Jahn-Teller (JT) distortions; as a consequence, a one-orbital approximation has been frequently used since the earliest theoretical studies (*6*). For these reasons, typical electronic models for the manganites include at least a kinetic energy contribution for the e_g electrons, regulated by hopping amplitude t, and a strong J_H coupling contribution between the e_g and t_{2g} spins. The localized spin is large enough (3/2) to be approximated by a classical spin, which simplifies the calculations. Here this model is simply referred to as the one-orbital model, although other names, such as FM Kondo model, are sometimes used.

This formalism leads to a natural explanation for the FM phase of the manganites, because carriers energetically prefer to polarize the spins in their vicinity. When an e_g electron jumps between nearest-neighbor ions, it does not pay an energy J_H if all the spins involved are parallel. The hole-spin scattering is minimized in this process, and the kinetic energy of the mobile carriers is optimized. This mechanism is usually referred to as double exchange (DE) (*6, 7*). As the carrier density grows, the FM distortions around the holes start overlapping and the ground state becomes fully FM.

Currently there is not much controversy about the qualitative validity of DE to stabilize a FM state. However, several experimental results suggest that more complex ideas are needed to explain the main properties of manganese oxides. For instance, above T_C and for a wide range of densities, several manganites exhibit insulating behavior of unclear origin that contributes to the large MR results. The low-temperature (T) phase diagram of these materials has a complex structure (*3*), not predicted by DE, that includes insulating AF and CO phases, orbital ordering, FM-insulating regimes, and, as discussed extensively below, tendencies toward formation of charge inhomogeneities, even within the FM phase. To address the strong MR effects and the overall phase diagram of manganites, the DE framework must be supplemented with more refined ideas.

Phase Separation in the One-Orbital Model

There has been considerable theoretical work, motivated by experimental research on manganese oxides, in the analysis of models for these materials. Several many-body techniques for modeling strongly correlated electron systems were developed and improved during recent efforts to understand high-temperature superconductors; thus, it is natural to apply some of these methods to manganite models. Of particular relevance here are the computational techniques that allow unbiased analysis of correlated models on finite clusters (*8*). The first comprehensive computational analysis of the one-orbital model was presented by Yunoki *et al.* (*9*), who used classical spins for the t_{2g} electrons and the Monte Carlo (MC) technique. Several unexpected results were found in this study. In particular, when the density of e_g electrons $\langle n \rangle = (1 - x)$ was being calculated as the chemical potential μ was varied, it was surprising that some densities could not be stabilized; in other words, $\langle n \rangle$ was found to

National High Magnetic Field Lab and Department of Physics, Florida State University, Tallahassee, FL 32306, USA.

change discontinuously at special values of μ. These densities are referred to as unstable. Alternative calculations in the canonical ensemble (*9, 10*), where the density is fixed to arbitrary values rather than being regulated by μ, showed that, at unstable densities, the resulting ground state is not homogeneous but is separated into two regions with different densities. The two phases involved correspond to those that bound the unstable range of densities (*9–11*). This phenomenon, which has been named phase separation (PS), appears in many contexts, such as the familiar liquid-vapor coexistence in the phase diagram of water, and it is associated with violation of the stability condition $\kappa^{-1} = \langle n\rangle^2\delta^2E/\delta\langle n\rangle^2 > 0$, where E is the energy of the system per unit volume and κ is the compressibility.

In the realistic limit $J_H/t \gg 1$, PS occurs between hole-undoped $\langle n\rangle = 1$ and hole-rich $\langle n\rangle < 1$ phases (*9–11*). Although the e_g and t_{2g} spins of the same ion tend to be parallel at large J_H, their relative orientation at one lattice spacing depends on the density. At $\langle n\rangle = 1$, an AF arrangement results because the Pauli principle precludes movement of the electrons if all spins are aligned. However, at stable $\langle n\rangle < 1$ densities, DE forces the spins to be parallel, as computer studies have indicated (*9–11*). Yunoki and Moreo (*11*) have shown that if an additional small Heisenberg coupling among the localized spins is introduced, PS occurs also at small $\langle n\rangle$, this time involving FM ($\langle n\rangle > 0$) and electron-undoped AF states. Phase segregation near the hole-undoped and fully doped limits implies that a spin-canted state (*6*) for the one-orbital model is not stable. Others arrived at similar conclusions after observing phase segregation tendencies by several analytical techniques (*12–14*). If a spin-canted state is unequivocally found in experiments, mechanisms other than that of DeGennes (*6*) may be needed to explain it. Note also that a canted state is difficult to distinguish experimentally from a mixed AF-FM state.

It is interesting that PS behavior is not unique to manganese oxides. Indeed, the existence of PS in AF rare-earth compounds has been addressed by Nagaev for many years (*15*). In these materials, there is a small density of electrons interacting with localized spins. Actually, $Eu_{1-x}Gd_xSe$ has a very large MR effect similar to that observed in manganites (*16, 17*). Calculations in this context were performed with the one-orbital model mainly in the limit where the localized-conduction spin-spin coupling is smaller than the bandwidth (equivalent to $J_H \ll t$) and at small $\langle n\rangle$. Nevertheless, some of these results have been discussed also in the context of manganites (*18*). Note that in the recently established phase diagram of the one-orbital model, PS occurs at both high and low electronic density (*11*). Because the $\langle n\rangle \ll 1$ limit corresponds to the dilute AF semiconductors mentioned above, the computational studies confirm that these materials should also exhibit PS tendencies. A broad distribution of FM cluster sizes should be expected, with a concomitant distribution of electrons trapped in those clusters (*19*). Gavilano *et al.* (*20*) have recently reported a two-phase mixed regime in these materials that may be related to intrinsic PS tendencies. Analogous results were also observed in other diluted magnetic semiconductors (*21*). Analysis of experimental data in this context should certainly allow for the possibility of large-scale inhomogeneous states.

PS in the Two-Orbital Model

Most of the theoretical studies for manganites have been carried out using the one-orbital model, which certainly provides a useful playground for the test of qualitative ideas. However, quantitative calculations must necessarily include two active e_g orbitals per Mn ion to reproduce the orbital-ordering effects known to occur in these materials (*22*). In addition, it has been argued that dynamical JT effects cannot be neglected (*23*), and the electron-JT-phonon coupling λ should be important for the manganites.

Although computational studies accounting for JT phonons are in the early stages, some illustrative results are already available. Yunoki *et al.* (*24*) recently reported the low-temperature phase diagram of a two-orbital model with the MC method and they analyzed the results in a manner similar to the one-orbital case. The results are reproduced in Fig. 1 for a one-dimensional (1D) system at large Hund coupling. The phase diagram is rich and includes a variety of phases such as metallic and insulating regimes with orbital order. The latter can be uniform, with the same combination of orbitals at every site, or staggered, with combinations alternating between the even and odd sites of the lattice at $\langle n\rangle = 1$. Recently, our group observed that the density of states exhibits pseudogap behavior caused by the PS tendencies, in both the one- and two-orbital cases, in agreement with photoemission experiments for layered manganites (*25*). Of special importance for the discussion here are the regions of unstable densities. PS appears at small e_g densities between an electron-undoped AF state and a metallic uniform-orbital-ordered FM state. The latter phase itself coexists at larger densities and intermediate values of λ with an insulating ($\langle n\rangle = 1$) staggered-orbital-ordered FM state in an orbital-induced PS process (*24*). The overall results are qualitatively similar to those obtained with other model parameters and in studies of two- and three-dimensional (2D and 3D) systems. Overall, PS tendencies are strong in both the one- and two-orbital models and over a wide range of couplings. Similar tendencies have been recently observed including large on-site Hubbard interactions (*26*), which is reasonable because at intermediate and large electron-phonon coupling a negligible probability of on-site double-occupancy was found (*24*).

The macroscopic separation of two phases with different densities, and thus different charges, should actually be prevented by long-range Coulombic interactions, which were not incorporated into the one- and two-orbital models discussed thus far. Even including screening and polarization effects, a complete separation leads to a huge energy penalty. This finding immediately suggests that the two large regions involved in the process will break into smaller pieces to spread the charge more uniformly. These pieces are hereafter referred to as polarons if they consist of just one carrier in a local environment that has been distorted by its presence. This distortion can involve nearby spins (magnetic polaron), nearby ions (lattice polaron), or both, in which case this object is simply referred to as a polaron. However, the terms clusters and droplets are reserved for extended versions of the polarons, characteristics of a PS regime, containing several car-

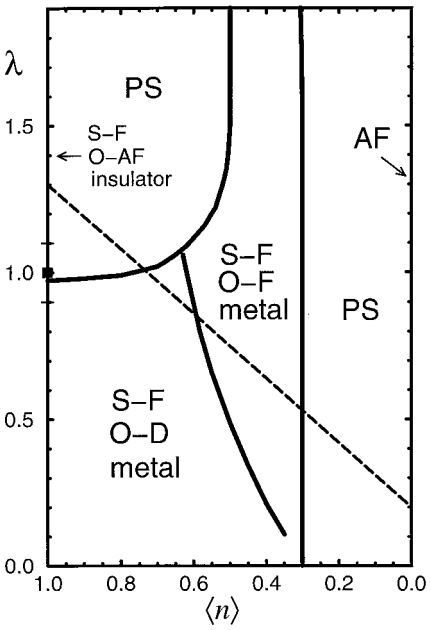

Fig. 1. Phase diagram of the two-orbital model for manganites in 1D and $T \sim 0$ including JT phonons, obtained with MC techniques (*24*). S-F labels a spin-FM configuration; O-F, O-AF, and O-D denote a state where the orbital degrees of freedom are ordered uniformly, staggered, or disordered, respectively; PS indicates a phase separated state, and AF is an anti-FM state. Hund coupling is $J_H = 8$ and Heisenberg coupling between localized classical spins is $J' = 0.05$, both in units of the hopping among the same orbitals. Meaning of the dashed line is explained in the text.

riers inside a common large magnetic distortion or lattice distortion, or both.

This discussion suggests that in the regime of unstable densities the inclusion of extended Coulomb interactions will lead to a stable state, with clusters of one phase embedded in the other [see also (*15*)]. It is expected that the competition between the attractive DE tendencies among carriers and the Coulomb forces will determine the size and shape of the resulting clusters. Either sizable droplets or polarons may arise as the most likely configuration (*27*). The stable state resulting from the inclusion of extended Coulomb interactions on an otherwise PS unstable regime is referred to as a charge-inhomogeneous (CI) state. However, the ideas presented here are still described as the PS scenario, with the understanding that only microscopic phase segregation is the resulting net effect of the DE-Coulomb competition. Related ideas have been discussed in the context of the cuprates (*28*), with attractive interactions generated by antiferromagnetism or phonons. An exception to the existence of only purely microscopic effects occurs if the competing phases have about the same density, as observed experimentally at $x = 0.5$ (discussed below). In this case, large-scale PS can be expected. Note also that the CI state is certainly different from the metastable states that arise in a standard first-order transition. Figure 2 presents a cartoon-like version of possible charge arrangements in the CI state, which are expected to fluctuate in shape, especially at high temperature where the clustering is dynamic. Unfortunately, actual calculations supporting a particular distribution are still lacking. Nevertheless, the currently available results are sufficient to establish dominant trends and to allow a qualitative comparison between theory and experiment, as shown below.

PS in manganese oxides has clear similarities with the previously discussed charge inhomogeneities observed in copper and nickel oxides (*28*). Actually, studies of 1D generalizations of the *t-J* model by Riera *et al*. (*29*), a model widely used to describe electrons in high-temperature superconductors, showed that as the localized spin magnitude S grows, the phase diagram is increasingly dominated by either FM or PS tendencies. The importance of PS arises from the dominance of the Heisenberg interactions over the kinetic energies as S increases, which causes holes to be expelled from the AF regions because they damage the spin environment. The tendency toward phase segregation decreases across the transition metal row, from a strong tendency in Mn to a weak tendency in Cu (*29*). The stripes observed in cuprates (*28*) could certainly appear in manganites as well through the competition of the DE attraction and Coulomb repulsion among clusters.

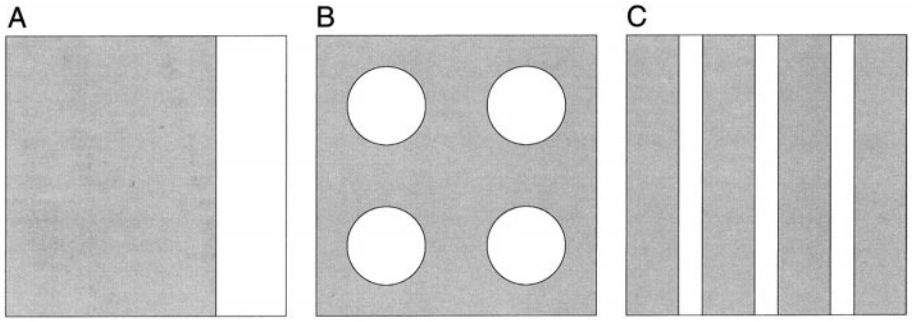

Fig. 2. Qualitative representation of a macroscopic phase-separated state (**A**) as well as possible CI states stabilized by extended Coulomb interactions, such as spherical droplets (**B**) or stripes (**C**). Diameter of droplets and stripes are expected to be microscopic, but realistic calculations are still lacking.

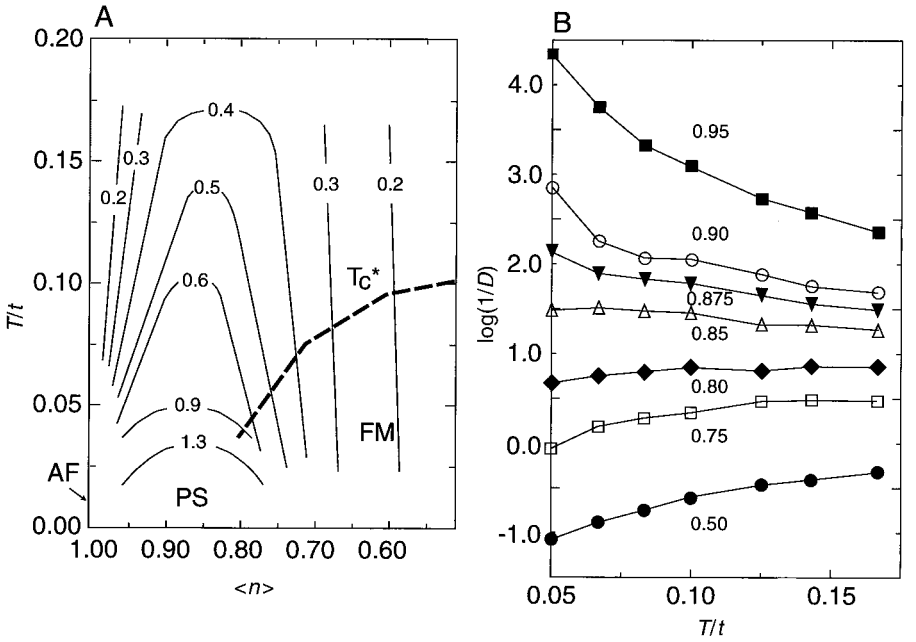

Fig. 3. (**A**) Lines of constant $\kappa\langle n\rangle^2 = d\langle n\rangle/d\mu$ that correspond to the one-orbital model with $J_H = \infty$ in the plane temperature $\langle n\rangle$ (e_g density). Plots were obtained from MC simulations with a 30-site chain with periodic boundary conditions. Coupling among the localized t_{2g} spins is $J' = 0.05t$ and t is the hopping amplitude. T_C^* is a characteristic temperature where the zero-momentum Fourier-transform of the spin-spin correlations starts growing very rapidly as the temperature is reduced (*9–11*). (**B**) Plot of log(1/*D*) versus *T*/*t* for the same model and cluster as in (A). *D* is the Drude weight obtained from the optical conductivity (*11*). Densities are indicated.

Influence of PS on the FM Phase

A critical aspect of the scenario discussed here is the influence of the low-temperature PS regime on the behavior of electrons at higher temperatures, especially on the ordered phases that neighbor PS regimes. As an illustration, consider the lines of constant $\kappa\langle n\rangle^2 = d\langle n\rangle/d\mu$ of the 1D one-orbital model at large J_H (Fig. 3A). Because PS occurs through the divergence of κ, naturally this quantity is largest at those densities where PS is observed (see above). A large κ implies that strong charge fluctuations occur, because $\kappa \propto (\langle N^2\rangle - \langle N\rangle^2)$, where N is the total number of particles. A characteristic crossover temperature for ferromagnetism T_C^* occurs where the zero-momentum spin structure factor starts growing very rapidly as the temperature is reduced. T_C^* is expected to become truly critical in higher dimensional systems, where a finite critical temperature for PS also is expected to exist. Figure 3A shows that the PS tendencies influence the neighboring FM state because the compressibilities close to the PS regime, located at $0.8 \leq \langle n\rangle \leq 1.0$, are much larger than those at, for example, $\langle n\rangle = 0.5$. This result implies that, even within the FM phase, which is uniform when time-averaged, there is a dynamical tendency toward cluster formation because κ is large.

The same situation occurs for $T > T_C^*$ and at low hole densities.

This effect should influence transport properties, including resistivity. Although it is difficult to evaluate ρ with finite-cluster techniques, crude estimations can be made by using the inverse of the zero-frequency Drude weight found from the optical conductivity (*11*). As an example, results are shown in Fig. 3B for the one-orbital model. This estimation of ρ produces the qualitatively expected results—namely, it behaves as an insulator at small x and rapidly decreases as x increases, turning smoothly into a metal. Studies by our group using more sophisticated techniques connecting the cluster with ideal metals have recently produced qualitatively similar data. The results compare well with experiments for Sr-doped compounds (*30*). Starting from a regime with dynamical cluster formation above T_C, the metallic state can be obtained if the clusters grow in size as T is reduced, eventually reaching the limit where percolation is possible. At this temperature, the carriers move over long distances and the metallic state is reached. The same mechanism arises in polaronic theories (*31*) [see also (*32*)].

Comparing Theory with Experiments: Phase Diagrams

The computational results are consistent with several experiments on a variety of manganese oxides. Consider, for example, $La_{1-x}Sr_xMnO_3$. The experimentally observed sharp increase in ρ as x decreases toward the undoped limit, both above and below T_C (*30*), is difficult to explain if the only effect of the correlations were to induce a reduced effective electronic hopping $t_{eff} = t\langle\cos(\theta/2)\rangle$, where θ is the angle between nearest-neighbor sites (*6*). In addition, the insulating properties of the intermediate region $0.0 < x < 0.16$ (*30*) do not fit into the simpler versions of the DE ideas. This regime is important because the CMR effect is maximized at the lowest T_C—that is, at the boundary between the metallic and insulating regions. Note also that recent experiments (*33, 34*) for hole densities slightly above $x = 0.5$ showed that the ground state of the (La,Sr)-based manganese oxide is an A-type AF metal with uniform $d_{x^2-y^2}$ orbital order (Fig. 4A). This phase, as well as the orbital-ordered $x = 0$ A-type AF insulator, does not appear in the one-orbital model (*9*). For these reasons, $La_{1-x}Sr_xMnO_3$ does not appear to be a typical DE material when considered including all available densities, although Furukawa (*35*) showed that it has DE characteristics at $x \sim 0.3$.

However, the experimental results mentioned above can be more naturally accounted for once PS tendencies and coupling with JT phonons are considered (narrower band materials are more complicated because of their $x = 0.5$ CO state, and they are discussed below). Actually, it has already been argued that ρ should rapidly grow as x decreases because of the strong charge fluctuations at small x caused by the nearby phase segregation regime (Fig. 3B). In this context, the insulating state above T_C of the lightly hole-doped (La,Sr)-compound can be rationalized as formed by clusters of one phase (FM or AF) embedded into the other. Even the experimentally observed A-type AF metallic $d_{x^2-y^2}$-ordered phase at $x \sim 0.5$ (Fig. 4A) can be related to the phase with similar characteristics near $x = 0.5$ found in the theoretical calculations (Fig. 1). Although simulations with the realistic hopping amplitudes needed to stabilize an A-type AF state in a 3D environment have not been performed yet, at least the 1D and 2D FM tendencies as well as stabilization of a uniform orbital ordering (Fig. 1) are clear. If phenomenologically one assumes that λ/t decreases with hole doping, the dashed line in Fig. 1 runs through the proper series of experimentally observed phases (*33*)—namely, an insulating staggered orbital-ordered state at $x = 0$, a charge-segregated regime at small x, a metallic orbital-disordered FM phase at a higher density, and finally the $x \sim 0.5$ orbitally ordered FM state compatible with A-type AF order in dimensions $D < 3$ (*36*). If it were possible to complete the phase diagram of $La_{1-x}Sr_xMnO_3$ by synthesizing $x > 0.6$ samples, the calculations predict a new mixed phase, involving the A-type AF metal with $x < 1$ and a G-type AF insulator with $x = 1$, where large MR effects potentially could occur.

Experimental Evidence of Charge Inhomogeneities

Independently of the development of theoretical ideas on PS, a large body of experimental evidence has accumulated that suggests the existence of charge inhomogeneities in manganese oxides either in macroscopic form or, more often, through the presence of small clusters of one phase embedded into another. The results have been obtained on several materials, at a variety of temperatures and densities, and using a large array of microscopic and macroscopic experimental techniques. These studies have individually concentrated on particular parameter regions, and the results have rarely been discussed in comparison to similar results obtained in other phase regimes. However, once all these experimental data are combined, it appears that the manganite metallic FM phase is surrounded in both temperature and density by CI regions involving FM clusters coexisting with another phase, which in some cases is AF. It would be unnatural to search for special justifications for each of these experimental results. The most economical hypothesis is to explain the data as arising through a single effect, such as tendencies to PS that compete strongly with ferromagnetism at both large and small x, as well as above T_C. The experimental details follow.

Sr-doped manganese oxides. Part of the phase diagram of $La_{1-x}Sr_xMnO_3$ is schemat-

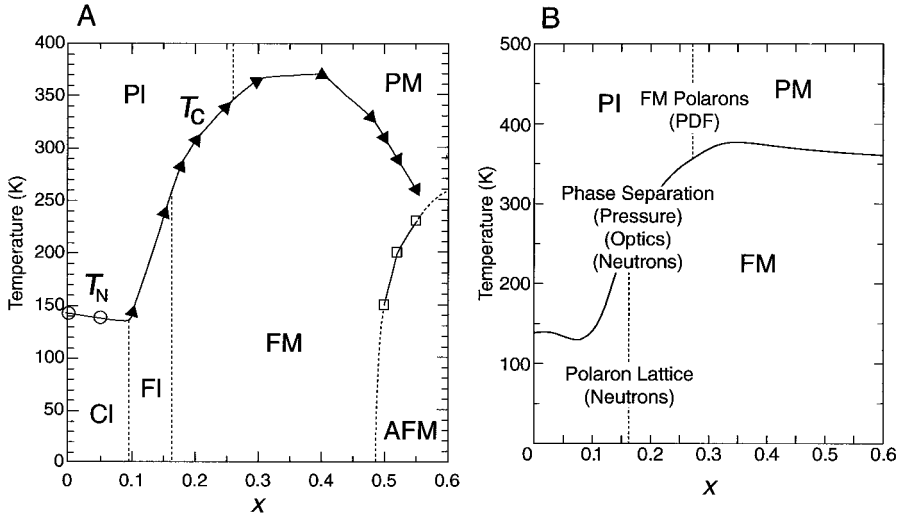

Fig. 4. (**A**) Phase diagram of $La_{1-x}Sr_xMnO_3$ (courtesy of Y. Tokura and Y. Tomioka) prepared with data from (*30*) and (*68*).The AFM phase at large x is an A-type AF metal with uniform orbital order. In this material there is no CO AF state near $x = 0.5$. PM, PI, FM, FI, and CI denote paramagnetic metal, paramagnetic insulator, FM metal, FM insulator, and spin-canted insulator states, respectively. T_C is the Curie temperature and T_N is the Néel temperature. (**B**) Schematic version of the phase diagram of $La_{1-x}Sr_xMnO_3$ to illustrate the experimental observation of the tendencies for charge inhomogeneities in this material. The language used to describe these tendencies, and the experimental techniques used, are indicated at the proper densities and temperatures. Additional details and references are in the text.

ically shown in Fig. 4B, including at the proper location in temperatures and densities some of the descriptions of charge inhomogeneity found in the literature, along with the experimental techniques that have reported such inhomogeneity. They include results by Egami *et al*. (*31*), where evidence for an inhomogeneous FM state and small polarons at both high and low T was reported using pair-density functional techniques. In addition, a recent analysis of the optical conductivity of $La_{7/8}Sr_{1/8}MnO_3$ by Jung *et al*. (*37*) observed PS features in the data. Magnetic, transport, and neutron-scattering experiments by Endoh *et al*. (*26*) on $La_{0.88}Sr_{0.12}MnO_3$ revealed PS tendencies between two FM phases, one metallic and the other insulating. Others have also reported inhomogeneities in Sr-doped compounds (*38*).

Ca-doped manganese oxides. The phase diagram of $La_{1-x}Ca_xMnO_3$ is sketched in Fig. 5. Although previous reports (*3*) contain more details, only the dominant qualitative aspects are needed for this discussion. The list of references is not exhaustive but it is sufficient to illustrate the notorious presence of charge inhomogeneities in this compound near the FM phase and even inside it. Overall, the analysis of available data for Ca-doped $LaMnO_3$ leads to conclusions similar to those presented for their Sr-doped counterpart.

The details are the following (postponing the analysis for $x \sim 0.5$, which requires special discussion). Consider first the small-angle neutron-scattering (SANS) results at $x = 0.05$ and 0.08 and at low T by Hennion *et al*. (*39*). They revealed the existence of a liquid-like distribution of FM droplets with a density 1/60th that of holes. In a similar regime of parameters, nuclear magnetic resonance experiments by Allodi *et al*. (*40*) reported the coexistence of FM and AF features and the absence of spin canting (*41*). SANS results at $x = 1/3$ and $T > T_C$ by Lynn *et al*. (*42*) and De Teresa *et al*. (*43*) observed a short (weakly T-dependent) FM correlation length, attributed in (*43*) to magnetic clusters 10 to 20 Å in diameter. Other experimental results, not reviewed here, agree with this conclusion. Even within the metallic FM phase ($T < T_C$), indications of charge inhomogeneities have been reported. Transport measurements by Jaime *et al*. (*44*) were analyzed with a two-fluid picture involving polarons and free electrons. The μ-spin relaxation and resistivity data of Heffner *et al*. (*45*) were interpreted as produced by a multidomain sample. X-ray absorption results of Booth *et al*. (*46*) provided evidence of coexisting localized and delocalized holes below T_C (*47*). Using Raman and optical spectroscopies, Yoon *et al*. (*17*) found localized states in the low-T metallic FM phase of several manganese oxides. Neutron scattering experiments (*42*) reported an anomalous diffusive component in the data below T_C, which could be explained by a two-phase state. Fernandez-Baca *et al*. (*48*) have shown that this diffusive component is enhanced as the T_C of the considered manganite decreases. Actually, the low-energy component of the two-branch spin-wave spectrum observed at small x (*49*) has similarities with the diffusive peak at $x = 1/3$ (*42*).

For the large hole-density regime, neutron scattering by Bao *et al*. (*50*) at $x \sim 0.8$ using $Bi_{1-x}Ca_xMnO_3$, which behaves similarly to $La_{1-x}Ca_xMnO_3$, revealed FM-AF features coexisting between 150 and 200 K. Optical measurements at $x > 0.5$ by Liu *et al*. (*51*) reported similar features. Cheong and Hwang in (*3*) found a finite magnetization at low T and $x \geq 0.83$ in the (La,Ca) compound [see also (*52*)]. The system remains insulating, and the results could be compatible with spin-canted or mixed-phase states. More work at small electronic density is needed to clarify whether the phase segregation predicted by the theoretical calculations indeed appears in experiments.

Manganese oxides with a CO state near $x = 0.5$. Results involving the CO AF state at $x \sim 0.5$ require special discussion. Here, the extraordinarily large CMR effect involves abrupt destabilization of the CO state by a magnetic field (*5*). Evidence for PS tendencies is rapidly accumulating in this region of the phase diagram of narrow-band manganese oxides. Several experiments for $La_{1-x}Ca_xMnO_3$ have already reported coexisting metallic FM and insulating CO-AF clusters near $x = 0.5$ (Fig. 5) (*53*). Another compound at the FM-CO boundary at low T is $Pr_{0.7}Ca_{0.3}MnO_3$. Here x-ray synchrotron and neutron-powder diffraction results (*54, 55*) were attributed to the presence of FM clusters in the CO phase. Exposure to x-rays produces a nonuniform PS phenomenon characteristic of two competing states, with an increasing size of the FM droplets and no evidence of spin canting. This phenomenon is expected to appear at other hole densities as well. Related manganese oxides exhibit similar features. For example, the absorption spectra of thin films of $Sm_{0.6}Sr_{0.4}MnO_3$ have been attributed (*32*) to the formation of large clusters of the CO state above its ordering temperature. In $(La_{0.5}Nd_{0.5})_{2/3}Ca_{1/3}MnO_3$, insulating CO and metallic FM regions coexist (*56*).

However, consider ρ at 300 K for $La_{1-x}Ca_xMnO_3$ (*3*). A smooth connection between the undoped, lightly doped, and heavily doped compounds appears to exist even in this narrow-band material. No obvious precursors for $x \geq 0.5$ of the low-T CO state have been reported. The same occurs for $Nd_{0.5}Sr_{0.5}MnO_3$, which is metallic above T_C, becomes FM upon cooling, and reaches the CO state through a first-order transition upon further decreasing T (*57*). These results establish a possible qualitative difference between the MR effect at small x and at $x \sim 0.5$. In the former, charge inhomogeneities appear above and below the critical temperatures, and the mutual influence of neighboring phases (notably FM and PS) is important. However, at $x \sim 0.5$, the CO and FM states do not appear to have much influence on each other. It could even be that the low-T microscopic PS tendencies at $x \sim 0.5$ may be caused by metastabilities rather than a stable CI state. However, because the competing states at $x \sim 0.5$ have similar $\langle n \rangle$, charge inhomogeneities involving large clusters are possible because Coulomb interactions will not prevent their formation (see above). Further experimental work is needed to clarify the situation. The theoretical study of competing FM and CO-AF states of narrow-band manganese oxides in a single formalism also represents a challenge for computational studies. Preliminary results are promising as a CE-type CO state has been recently stabilized in computer simulations carried out at large electron-phonon coupling (*58*).

Layered manganites. Tendencies toward PS in layered manganites have also been observed. Neutron scattering results (*59*) for the bilayered $La_{1.2}Sr_{1.8}Mn_2O_7$ revealed a weak peak at the AF momentum of the parent compound that coexists with the dominant FM signal (*60*).

Recently, PS between A-type metallic and

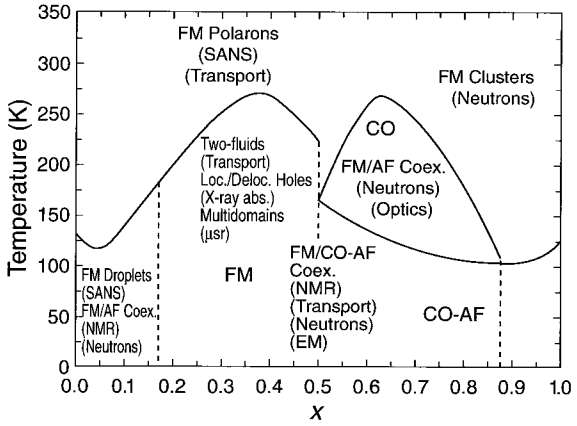

Fig. 5. Schematic version of the phase diagram for $La_{1-x}Ca_xMnO_3$ [see (*3*)]. Some of the experiments listed were performed for $Bi_{1-x}Ca_xMnO_3$, the bismuth analog. Coex., Loc., Deloc., abs., μsr, and EM designate coexistence, localized, delocalized, absorption, muon spin relaxation, and electron microscopy, respectively.

CE-type insulating CO states was reported for $La_1Sr_2Mn_2O_7$ (*61*). In addition, studies of the one-layer material $Sr_{2-x}La_xMnO_4$ (*62*) found direct evidence for macroscopic PS at small electronic density (*63*).

PS Scenario Compared with Other Theories for Manganites

The PS scenario is qualitatively different from other theories proposed to explain the CMR effects in manganese oxides. It improves on the simpler versions of the DE ideas (*6*) by identifying charge inhomogeneities as the main effect competing with ferromagnetism and by assigning the insulating properties above T_C, fundamental for the low hole-density CMR effect, to the influence of those competing phases. In particular, the compressibility increase above T_C caused by PS leads to dynamical cluster formation.

The ideas presented here also differ qualitatively from those of Millis *et al*. (*23*), although there are common aspects. In the PS scenario, charge inhomogeneities over several lattice spacings, not contained in local mean-field approximations (*23*), are believed to be relevant for description of the insulating state above T_C. In addition, orbital ordering plays a key role in the results presented in Fig. 1. Although the importance of the JT coupling introduced by Millis *et al*. (*23*) is shared in both approaches, in the PS scenario a state formed by independent local polarons is a special case of a more general situation where clusters of various sizes and charges are possible. These fluctuations increase as T_C decreases, explaining the optimization of the MR effect at the boundary of the FM phase. Note that the regime of small x is crucial to distinguish between the PS scenario and other polaronic theories based on more extended polarons and percolative processes (*31*).

Other theories are based on the electronic localization effect using the off-diagonal disorder intrinsic to the DE model (*64*) and the nonmagnetic diagonal disorder caused by the chemical substitutions. These effects lead to a large MR under some approximations (*65*). However, the calculations are difficult because they involve both strong couplings and disorder, and the prominent cluster and polaron formation found in experiments has not been addressed in this framework. A better starting point for manganites may need a formalism that accounts for the tendency to develop charge inhomogeneities before including disorder.

Conclusions

A variety of recent calculations has found PS tendencies in models for manganites, usually involving FM and AF phases. These tendencies, which should lead to a stable but microscopically inhomogeneous state upon inclusion of Coulomb interactions, compete strongly with ferromagnetism in the phase diagrams and are expected to substantially increase the resistivity. Particularly, when two-orbital models are studied, the results are in good agreement with a large list of experimental observations reviewed here. Tendencies toward CI states exist in real manganese oxides all around the FM phase in the temperature-density phase diagram. The computer simulations have shown that the region with PS tendencies substantially influences the stable FM phase by increasing its compressibility, an aspect that can be tested experimentally. This provides a rationalization for experimental observation of a large MR effect at the boundaries of the FM phase. The presence of short-range charge correlations is certainly a crucial feature of the PS scenario.

However, considerable work still remains to be done. The inclusion of extended Coulomb interactions and the stabilization of the $x = 0.5$ CO state are the next challenges for computational studies. Analytical techniques beyond the local mean-field approximations are needed to capture the essence of the CI state. Macroscopic phenomenological approaches should be used to obtain predictions for transport properties and the shapes of the clusters that arise from the competition of the DE attraction and Coulomb repulsion. These resulting clusters are surely not static but fluctuating, especially above T_C. In related problems of nuclear physics at high density, several geometries have been found, including spherical drops, rodlike structures [stripes (*28*) or spaghetti], and platelike structures [lasagna (*66*)]. Similar rich phenomena may occur in manganites. On the experimental front it is crucial to establish whether the various regimes with charge inhomogeneities (Figs. 4B and 5) are related, as predicted by the theoretical calculations. For example, work should be carried out to link the small x regime of (La,Ca) manganites where FM droplets appear, with the polarons reported at the $x = 1/3$ density, and beyond into the highly hole-doped regime. In addition, phase segregation tendencies should also be studied close to the fully doped limit $\langle n \rangle \ll 1$ of manganese oxides as well as in related compounds such as doped AF semiconductors (*67*).

References and Notes

1. Y. Tokura *et al.*, *J. Appl. Phys*. **79**, 5288 (1996); A. P. Ramirez, *J. Phys. Condens. Matter* **9**, 8171 (1997); Y. Tokura, in *Colossal Magnetoresistance Oxides*. *Monographs in Condensed Matter Science*, Y. Tokura, Ed. (Gordon & Breach, Reading, UK, in press); J. M. D. Coey, M. Viret, S. von Molnar, *Adv. Phys*., in press.
2. S. Jin *et al.*, *Science* **264**, 413 (1994).
3. P. Schiffer *et al.*, *Phys. Rev. Lett*. **75**, 3336 (1995); S-W. Cheong and H. Y. Hwang, in *Colossal Magnetoresistance Oxides. Monographs in Condensed Matter Science*, Y. Tokura, Ed. (Gordon & Breach, Reading, UK, in press); see also A. P. Ramirez *et al.*, *Phys. Rev. Lett*. **76**, 3188 (1996).
4. J. Goodenough, *Phys. Rev*. **100**, 564 (1955); see also T. Mizokawa and A. Fujimori, *Phys. Rev. B* **56**, R493 (1997), and references therein.
5. Y. Tomioka *et al.*, *J. Phys. Soc. Jpn*. **64**, 3626 (1995); *Phys. Rev. B* **53**, R1689 (1996); H. Yoshizawa *et al.*, *ibid*. **52**, R13145 (1995).
6. P. G. de Gennes, *Phys. Rev*. **118**, 141 (1960) and references therein.
7. C. Zener, *ibid*. **82**, 403 (1951).
8. E. Dagotto, *Rev. Mod. Phys*. **66**, 763 (1994).
9. S. Yunoki *et al.*, *Phys. Rev. Lett*. **80**, 845 (1998).
10. E. Dagotto *et al.*, *Phys. Rev. B* **58**, 6414 (1998).
11. S. Yunoki and A. Moreo, *ibid.*, p. 6403.
12. D. Arovas and F. Guinea, *ibid.*, p. 9150; M. Y. Kagan *et al*., abstract available at http://xxx.lanl.gov/abs/cond-mat/9804213; D. Arovas, G. Gomez-Santos, F. Guinea, abstract available at http://xxx.lanl.gov/abs/cond-mat/9805399.
13. S-Q. Shen and Z. D. Wang, *Phys. Rev. B* **58**, R8877 (1998); H. Yi and J. Yu, *ibid.*, p. 11123; L-J. Zou, Q-Q. Zheng, H. Q. Lin, abstract available at http://xxx.lanl.gov/abs/cond-mat/9806015; M. Yamanaka, W. Koshibae, S. Maekawa, *Phys. Rev. Lett*. **81**, 5604 (1998).
14. E. L. Nagaev, *Phys. Rev. B* **58**, 2415 (1998).
15. _____, *Phys. Status Solidi B* **186**, 9 (1994) and references therein.
16. P. Nyhus *et al.*, *Phys. Rev. B* **56**, 2717 (1997).
17. S. Yoon *et al.*, *ibid.* **58**, 2795 (1998).
18. E. L. Nagaev, *Phys. Uspekhi* **39**, 781 (1996). The heterogeneity in mixed-valence manganites has also been recently mentioned in [S. von Molnar and J. M. D. Coey, *Curr. Opin. Solid State Mater. Sci*. **3**, 171 (1998); E. Dagotto, S. Yunoki, A. Moreo, abstract available at http://xxx.lanl.gov/abs/cond-mat/9809380, *Proc. Workshop Physics of Manganites*, Michigan State Univ., July 1998, T. A. Kaplan and S. D. Mahanti, Eds. (Plenum, New York, 1998).
19. This effect has already been observed (S. L. Cooper, personal communication).
20. J. L. Gavilano *et al.*, *Phys. Rev. Lett*. **81**, 5648 (1998); see also [J. L. Gavilano *et al.*, *Phys. Rev. B* **52**, R13106 (1995)].
21. T. Kasuya and A. Yanase, *Rev. Mod. Phys*. **40**, 684 (1968); S. von Molnar and S. Methfessel, *J. Appl. Phys*. **38**, 959 (1967); H. Ohno *et al.*, *Phys. Rev. Lett*. **68**, 2664 (1992).
22. Y. Murakami *et al.*, *Phys. Rev. Lett*. **80**, 1932 (1998); *ibid*. **81**, 582 (1998).
23. A. J. Millis, P. B. Littlewood, B. I. Shraiman, *ibid*. **74**, 5144 (1995); A. J. Millis, B. Shraiman R. Mueller, *ibid*. **77**, 175 (1996); see also H. Röder *et al.*, *ibid*. **76**, 1356 (1996).
24. S. Yunoki, A. Moreo, E. Dagotto, *ibid*. **81**, 5612 (1998).
25. D. S. Dessau *et al.*, *ibid*., p. 192.
26. Y. Endoh *et al.*, preprint; K. Kubo, D. M. Edwards, A. C. M. Green, T. Momoi, H. Sakamoto, preprint, abstract available at http://xxx.lanl.gov/abs/cond-mat/9811286; Y. Motome, H. Nakano, M. Imada, preprint, abstract available at http://xxx.lanl.gov/abs/cond-mat/9811221; Y. Motome and M. Imada, unpublished results; N. Nagaosa, personal communication.
27. Some numerical results already support this picture (A. Malvezzi, S. Yunoki, E. Dagotto, *Phys. Rev. B*, in press).
28. K. A. Müller and G. Benedek, Eds. *Proc. Conference on Phase Separation in Cuprate Superconductors* (World Scientific, Singapore, 1993); V. J. Emery and S. A. Kivelson, *Phys. C* **209**, 597 (1993); C. Castellani, C. Di Castro, M. Grilli, *Phys. Rev. Lett*. **75**, 4650 (1995); J. M. Tranquada *et al.*, *Nature* **375**, 561 (1995); E. Dagotto *et al.*, *Phys. Rev. B* **49**, 3548 (1994) and references therein [see also L. P. Gor'kov and A. Sokol, *JETP Lett*. **46**, 420 (1987)].
29. J. Riera, K. Hallberg, E. Dagotto, *Phys. Rev. Lett*. **79**, 713 (1997).
30. A. Urushihara *et al.*, *Phys. Rev. B* **51**, 14103 (1995).
31. T. Egami, *J. Low Temp. Phys*. **105**, 791 (1996); T. Egami *et al.*, *J. Supercond*. **10**, 323 (1997); D. Louca and T. Egami, *J. Appl. Phys*. **81**, 5484 (1997); D. Louca *et al.*, *Phys. Rev. B* **56**, R8475 (1997).
32. A. Machida, Y. Moritomo, A. Nakamura, *Phys. Rev. B* **58**, 12540 (1998).

33. T. Akimoto *et al., ibid.* **57**, R5594 (1998).
34. Note that the phase diagram of $Pr_{1-x}Sr_xMnO_3$ [H. Kawano *et al., Phys. B* **289**, 241 (1998); *Phys. Rev. Lett.* **78**, 4253 (1997); H. Yoshizawa *et al., Phys. Rev. B* **58**, R571 (1998)] also presents an A-type AF phase at $x \sim 0.5$. The same occurs in $Nd_{1-x}SrxMnO_3$, with the exception of a small window near $x = 0.5$, where a CO insulator is the ground state.
35. N. Furukawa, *J. Phys. Soc. Jpn*. **63**, 3214 (1994); *ibid*. **64**, 2754 (1995); *ibid*. **66**, 2523 (1997).
36. Similar results were reported within a mean-field approximation [R. Maezono, S. Ishihara, N. Nagaosa, *Phys. Rev. B* **57**, R13993 (1998)].
37. J. H. Jung *et al*., preprint, abstract available at http://xxx.lanl.gov/abs/cond-mat/9809107; see also K. H. Kim, J. H. Jung, T. W. Noh, *Phys. Rev. Lett*. **81**, 1517 (1998) and references therein.
38. J.-S. Zhou *et al., Phys. Rev. Lett*. **79**, 3234 (1997); Y. Yamada *et al., ibid*. **77**, 904 (1996); for a different interpretation, see L. Vasiliu-Doloc *et al., Phys. Rev. B* **58**, 14913 (1998); M. Viret *et al., Europhys. Lett*. **42**, 301 (1998); T. W. Darling *et al., Phys. Rev. B* **57**, 5093 (1998).
39. M. Hennion *et al., Phys. Rev. Lett*. **81**, 1957 (1998).
40. G. Allodi *et al., Phys. Rev. B* **57**, 1024 (1998).
41. Dynamic and static magnetic properties reported by Troyanchuk [I. O. Troyanchuk, *Sov. Phys. JETP* **75**, 132 (1992)] also found a mixed AF-FM state at low hole density.
42. J. W. Lynn *et al., Phys. Rev. Lett*. **76**, 4046 (1996); J. W. Lynn *et al., J. Appl. Phys*. **81**, 5488 (1997).
43. J. M. De Teresa *et al., Nature* **386**, 256 (1997); see also J. B. Goodenough and J.-S. Zhou, *ibid*. **386**, 229 (1997).
44. M. Jaime, P. Lin, M. B. Salamon, P. Dorsey, M. Rubinstein, abstract available at http://xxx.lanl.gov/abs/cond-mat/9808160; M. Jaime *et al., Phys. Rev. B* **54**, 11914 (1996).
45. R. H. Heffner *et al., Phys. Rev. Lett*. **77**, 1869 (1996).
46. C. H. Booth *et al., ibid*. **80**, 853 (1998); C. H. Booth *et al*., *Phys. Rev. B* **57**, 10440 (1998).
47. See also S. J. L. Billinge *et al., Phys. Rev. Lett*. **77**, 715 (1996); G. Zhao *et al., Nature* **381**, 676 (1996); T. A. Tyson, *Phys. Rev. B* **53**, 13985 (1996); A. Lanzara *et al., Phys. Rev. Lett*. **81**, 878 (1998).
48. J. A. Fernandez-Baca *et al., Phys. Rev. Lett*. **80**, 4012 (1998). Note, however, that in (*42*) the diffusive peak was not observed at $Ca(x) = 0.15$.
49. M. Hennion *et al., Phys. Rev. B* **56**, R497 (1997); F. Moussa *et al., Physica. B* **241**, 445 (1998).
50. W. Bao *et al., Phys. Rev. Lett*. **78**, 543 (1997). Related results, but for $Pr_{1-x}Ca_xMnO_3$, are in R. Kajimoto *et al., Phys. Rev. B* **58**, R11837 (1998).
51. H. L. Liu, S. L. Cooper, S-W. Cheong, *Phys. Rev. Lett*. **81**, 4684 (1998).
52. H. Chiba *et al., Solid State Comm*. **99**, 499 (1996).
53. G. Papavassiliou *et al., Phys. Rev. B* **55**, 15000 (1997); J. J. Rhyne *et al., J. Appl. Phys*. **93**, 7339 (1998); M. Roy *et al., Phys. Rev. B* **58**, 5185 (1998); S. Mori *et al., Phys. Rev. Lett*. **81**, 3972 (1998); P. Calvani *et al., ibid*. **81**, 4504 (1998); G. Allodi *et al., ibid*., p. 4736; P. Dai *et al*., preprint.
54. D. E. Cox *et al., Phys. Rev. B* **57**, 3305 (1998); see also H. Yoshizawa *et al., J. Phys. Soc. Jpn*. **65**, 1043 (1996).
55. V. Kiryukhin *et al., Nature* **386**, 813 (1997); D. Casa *et al*., preprint, abstract available at http://xxx.lanl.gov/abs/cond-mat/9809242.
56. M. R. Ibarra *et al., Phys. Rev. B* **57**, 7446 (1998). Thermoelectric power measurements on similar manganese oxides were also attributed to hole-rich clusters embedded in a hole-poor matrix [J.-S. Zhou and J. B. Goodenough, *Phys. Rev. Lett*. **80**, 2665 (1998)].
57. H. Kuwahara, Y. Tomioka, A. Asamitsu, Y. Moritomo, Y. Tokura, *Science* **270**, 961 (1995).
58. S. Yunoki, A. Moreo, E. Dagotto, unpublished data.
59. T. G. Perring *et al., Phys. Rev. Lett*. **78**, 3197 (1997). Transport analysis for the same material found FM polarons condensing into clusters on cooling [J.-S. Zhou, J. B. Goodenough, J. F. Mitchell, *Phys. Rev. B* **58**, R579 (1998)].
60. See also R. Osborn *et al., Phys. Rev. Lett*. **81**, 3964 (1998); S. Rosenkranz *et al., J. Appl. Phys*. **83**, 7348 (1998).
61. M. Kubota *et al*., preprint, abstract available at http://xxx.lanl.gov/abs/cond-mat/9811192.
62. W. Bao *et al., Solid State Comm*. **98**, 55 (1996).
63. Moritomo *et al*. [Y. Moritomo *et al., Phys. Rev. B* **51**, 3297 (1995)] reported a spin glass in the one-layer compound. Maignan *et al*. [A. Maignan *et al., Phys. Rev. B* **58**, 2758 (1998)] found a cluster glass in $Ca_{1-x}Sm_xMnO_3$. Both results may be caused by a mixed AF-FM state.
64. E. Müller-Hartmann and E. Dagotto, *Phys. Rev. B* **54**, R6819 (1996); C. M. Varma, *ibid.*, p. 7328; see also M. J. Calderon and L. Brey, *ibid.* **58**, 3286 (1998); M. J. Calderon, J. A. Vergés, L. Brey, abstract available at http://xxx.lanl.gov/abs/cond-mat/9806157.
65. L. Sheng *et al., Phys. Rev. Lett*. **79**, 1710 (1997); R. Allub and B. Alascio, *Phys. Rev. B* **55**, 14113 (1997); H. Aliaga, R. Allub, B. Alascio, abstract available at http://xxx.lanl.gov/abs/cond-mat/9804248.
66. See C. P. Lorenz, D. G. Ravenhall, C. J. Pethick, *Phys. Rev. Lett*. **70**, 379 (1993) and references therein.
67. Other materials have competing FM-AF states at a fixed density when the bandwidths are changed by chemical substitution. For example, $(La_{1-y}Tb_y)_{2/3}Ca_{1/3}MnO_3$ has FM and AF phases as y is varied, with a complicated intermediate regime [J. M. De Teresa *et al., Phys. Rev. B* **56**, 3317 (1997)]. Ruthenates such as $(Sr_{1-y}Ca_y)_3Ru_2O_7$ also have a FM-AF competition near $y = 0.5$ [G. Cao *et al., Phys. Rev. B* 56, 5387 (1997)]. In these intermediate regions PS phenomena potentially could occur.
68. H. Fujishiro *et al., J. Phys. Soc. Jpn*. **67**, 1799 (1998).

69. A.M. and E.D. are supported in part by grant NSF-DMR-9814350. Part of the ideas discussed here were developed in collaborations with N. Furukawa, J. Hu, and A. Malvezzi (*9*).The authors are especially thankful to W. Bao, S. J. Billinge, C. H. Booth, S. L. Cooper, T. Egami, A. Fujimori, N. Furukawa, J. Goodenough, M. Hennion, M. Jaime, J. Lynn, S. Maekawa, Y. Moritomo, J. Neumeier, T. W. Noh, G. Papavassiliou, P. G. Radaelli, A. Ramirez, P. Schiffer, Y. Tokura, and H. Yoshizawa for their important comments and criticism. We thank E. Fradkin for bringing (*66*) to our attention.